Structural and electronic properties of liquid boron from a molecular-dynamics simulation

N. Vast,* S. Bernard, and G. Zerah
Commissariat à l'Energie Atomique, Centre d'Etudes de Limeil-Valenton, 94195 Villeneuve-St-Georges Cedex, France
(Received 30 June 1994; revised manuscript received 10 March 1995)

An *ab initio* molecular-dynamics simulation of liquid boron is presented. At the density $\rho \sim 2$ g cm^{-3} and the temperature $T \sim 2600$ K, icosahedra are destroyed although atoms still form an open packing with sixfold coordination. Moreover, we found that most three-center covalent bonds, which make the α-rhombohedral phase semiconducting, are destroyed. Furthermore, the estimated conductivity shows that boron undergoes a semiconductor-to-metal transition on melting, in agreement with the scarce experimental information.

I. INTRODUCTION

Boron and boron compounds are widely used materials with numerous technological applications, peculiarly in those where a light and hard material is required. Isotopic boron has proven to be useful in electronics, medical applications, and of course in nuclear physics. Boron-rich solids hold a special place within chemistry. Their electronic structure is dominated by covalent bonding: the ionization potentials of boron are high and the total energy required to produce B^{3+} ions can be compensated neither by lattice energy of ionic compounds nor by hydration of such ions in solutions. Tendency to form a cation plays therefore no role in boron chemistry.

Moreover, despite the $2s^2 2p$ electronic structure, boron is never monovalent but trivalent, and possesses fewer valence electrons (3) than it has valence shell orbitals (4), which is referred to as electron deficiency. Boron forms a covalent semiconductor (as far as rhombohedral phases are concerned) by adopting unique structures surpassed only in complexity by sulfur among the elements.[1]

The structural chemistry of elemental boron is dominated by the regular icosahedron. Not less than 16 distinct allotropic phases have been listed. Most of them have a huge number of atoms per unit cell (>50) and well located structural holes.[2] In this regard, the distinction between pure boron and a boron-rich solid seems to be slight, as the former is exceedingly difficult to prepare because of both the high melting point and the corrosiveness of the liquid. Only recently was the high melting temperature [$T_m \sim 2360 \pm 10$ K (Ref. 3)] determined with a complete containerless process, and, to the authors' knowledge, no experimental characterization of structural or electronic properties of the liquid state is available.

It has been suggested[4] that only three pure boron phases (glassy boron, α-rhombohedral B_{12}, and tetragonal B_{192} crystals) have been prepared experimentally, the other solid phases being stabilized by the presence of impurity atoms.[4] The existence of tetragonal B_{50} is still a source of controversy where *ab initio* calculations[5] could confirm the initial experimental work of Amberger *et al.* The phase diagram of boron can be considered as largely unknown. The β-rhombohedral phase B_{105} is thought to be thermodynamically stable at all temperatures below melting, and α-rhombohedral B_{12} transforms into B_{105} around 1400 K.[6]

The simplest crystalline phase, α-rhombohedral B_{12}, is representive of the class of icosahedral-based structure. It appears as a slightly distorted face-centered-cubic arrangement of icosahedra. These are assembled in a highly rigid, yet quite open, three-dimensional framework. Six of the 12 atoms of each icosahedron are directly bonded to one atom of six neighboring icosahedron. Each atom also has five neighbors within its own icosahedron, so that the usual two-center bonding scheme fails because of electron deficiency. Intraicosahedral bonding can then be explained in terms of 13 bonding orbitals lying on the twenty faces of the icosahedron. The four remaining electrons are involved in three-center intericosahedral bonds. This unusual type of bonding leads to a semiconductor, each electron being engaged in covalent bonds.[7]

There are few theoretical studies on liquid boron. Within density functional theory, band structure methods relying on the atomic sphere approximation are not aimed at simulating such a low symmetry and open structure as rhombohedral boron, and pseudoatoms must be introduced in intersticial zones.[8] When dealing with ionic dynamics, construction of effective interatomic potentials derived from pseudopotentials are problematic for most second row elements, since the atomic core is not screened for p orbitals.[9]

Questions about the liquid state arise from the structural peculiarities of solid boron. The first question concerns the short range order and binding upon melting. The experimental volume expansion and the low surface tension of boron have lead to the speculation that the icosahedral structure might be preserved in the liquid.[10]

The second question concerns the strong electronic similarities between boron and other s-p bonded solids with a small gap such as silicon or germanium. Since, in general, boron chemistry resembles that of silicon more closely than that of heavier group-III elements, the question arises whether boron undergoes a similar semiconductor-to-metal transition upon melting, although it expands rather than contracts at the melting point.

To study the liquid phase, we have undertaken a constant volume, constant temperature molecular-dynamics study of liquid boron at $T^{\text{target}}=2600$ K slightly above its melting temperature. The density was $\rho\sim 2$ g cm^{-3} as the volume of boron was estimated to increase by 9.3% on melting.[11] Standard Bachelet-Hamann-Schlüter (BHS) pseudopotentials were first used to investigate atomic and electronic properties. We also used the softer Trouiller-Martins pseudopotential which allowed a faster convergence of total energy with the size of the plane wave basis set. The results using either representation are very similar, and BHS results were confirmed with this more accurate electronic description. The rest of the paper is organized as follows: in Sec. II, we describe the computational details. Section III is devoted to the atomic structural properties and to the bonding properties. Dynamical properties are then described in Sec. IV, and electronic properties are gathered in Sec. V. Conclusions from this study are given in Sec. VI.

II. COMPUTATIONAL DETAILS

A. Choice of a pseudopotential for boron

We first consider the standard norm-conserving Bachelet-Hamann-Schlüter (BHS) formulation as tabulated in Ref. 12 which has been used by Mailhot *et al.*[8] to study the high pressure metallic phases of boron. In that work, the stability of α-rhombohedral B_{12} relative to other hypothetical phases was well predicted. Tests have also shown that the use of a kinetic energy cutoff larger than 25 Ry simply leads to a rigid shift of the total energy curves as a function of atomic volume, while properties such as bulk modulus or equilibrium volume are preserved. Therefore, although the total energy is not completely converged, we might expect a correct description of interatomic forces since equilibrium properties are properly estimated. In our BHS simulation, we found that ionic dynamical properties were much more sensitive to the cutoff. For instance, the self-diffusion coefficient increases when a smaller cutoff is used, and caging effect of neighboring atoms on a central atom are not observed in the velocity autocorrelation function. We then undertook another simulation with the softer Trouiller-Martins (TM) pseudopotential.[13] In the later formalism, cutoff radii were chosen to be $r_c^{2s}=r_c^{2p}=1.85$ a.u., values which were used in determine electron momentum density in hexagonal boron nitride.[14]

B. Text of the BHS and TM pseudopotentials on the crystalline phase

The simulation of the liquid was performed in a cubic supercell, and the initial configuration was obtained by slightly distorting the experimental α-rhombohedral phase determined by Decker and Kasper. We have kept the rhombohedral angle ($\alpha=58°$) to generate icosahedra which were then packed in a perfect fcc lattice ($\alpha=60°$). The supercell contained 48 boron atoms with simple cubic periodic boundary conditions. At the solid density ($\rho=2.46$ g cm^{-3}), intericosahedral two-center and three-center bond lengths were respectively shortened by 0.5% and enlarged by 7.0% with respect to experimental data.[2] Bond length are gathered in Table I.

TABLE I. Bond length in the experimental B_{12} unit cell[35] (d_{exp}), and in the supercell where icosahedra are packed on a perfect fcc lattice (see text, d_{fcc}). Only changes are indicated. The number N_b of bond length in one B_{12} unit cell is also given.

Type of bonds	N_b	$1d_{\text{fcc}}$ (Å)	$1d_{\text{exp}}$ (Å)
Two-center intericosahedra	6	1.702	1.709
Three-center intericosahedra	6	2.169	2.021
Intraicosaedron	6		1.733
	8		1.773
	8		1.785
	8		1.787

In our simulation the Kleinman and Bylander form was used with *s-p* nonlocality included for the BHS pseudopotential and only *s* nonlocality for TM pseudopotential. Electronic minimizations were performed using a cutoff energy between 15 and 50 Ry, and convergence is reached more rapidly when the TM pseudopotential is used. At 35 Ry, total energy of the supercell is converged within 0.4 eV (TM) and only within 10.5 eV (BHS) with respect to those obtained for the 50 Ry cutoff. In the later BHS case, Kohn-Sham eigenvalues are converged within ± 0.2 eV with respect to those obtained for the 50 Ry cutoff. The bandwidth (15.4 eV) compares well with the experimental one (15.5 eV).[15]

In order to check whether our pseudopotentials and a cutoff of 35 Ry yield correct values, we have compared the electronic charge densities with those obtained by Lee Bylander, and Kleinman.[16] We recall here that our structure is slightly distorted and that the only Γ point was

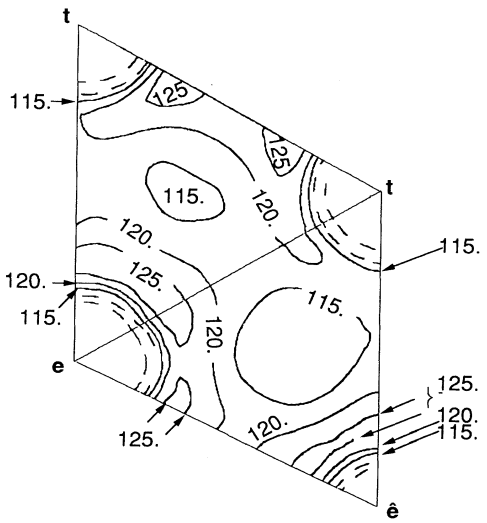

FIG. 1. Contours of constant charge density in steps of 5 me (millielectrons) per cubic bohr on two triangular face of an icosahedron. The faces are labeled (t,t,e) and $(t,e,\hat{e})$ in Ref. 16 (Fig. 4) (BHS results).

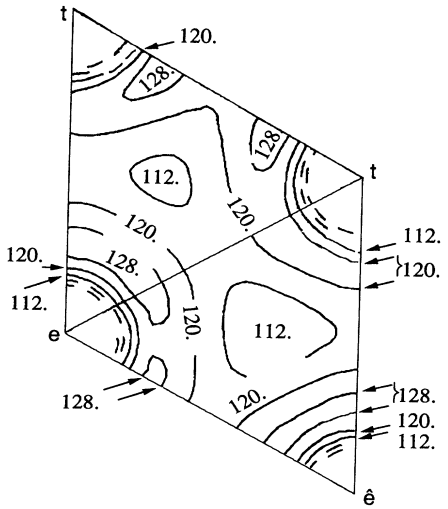

FIG. 2. Same as Fig. 1 for the TM pseudopotential. Contours of constant charge density are in steps of 8 me (millielectrons) per cubic Bohr.

used in the Brillouin zone of the supercell, whereas the work of Lee, Bylander, and Kleinman deals with the rhombohedral unit cell at the relaxed equilibrium lattice parameters and atomic positions, a different pseudopotential and 5 **k** points in the irreducible wedge of the Brillouin zone.

Dealing first with intericosahedral bonds and BHS pseudopotential, we found that the two-center intericosahedral bond has a double peak of 168 me/a_0^3 [resp. 160 me/a_0^3 (Ref. 16)]. Indeed, topology of the contours is in reasonable agreement with those obtained in Ref. 16; the mean difference is around 8 me/a_0^3 (54 me/Å^3). The three-center intericosahedral bond is the most distorted bond in our model, but it is interesting because Lee, Bylander, and Kleinman give details of the contributions to the charge density at the Γ point. We found a peak density of 83 me/a_0^3 [resp. 89 me/a_0^3 (Ref. 16)] and a bond center of 70 me/a_0^3 [resp. 73 me/a_0^3 (Ref. 16)].

We have then compared the electronic charge density at the surface of the icosahedron obtained with BHS and TM pseudopotentials. Contours of constant charge density in the plane of two triangular faces of an icosahedron [referred to as (t,t,e) and $(t,e,\hat{e})$ in [Ref. 16, Fig. 4], are shown Fig. 1 (BHS) and Fig. 2 (TM). In the former description, intraicosahedral bond is characterized by a density peak of 125 me/a_0^3, (resp. 128 me/a_0^3) and a much less symmetric topology. Moreover, values of charge density vary only within 1 me/a_0^3 when the cutoff is raised to 50 Ry for the BHS pseudopotential, whereas, in our distorted cell, TM pseudopotential clearly reproduces theoretical charge density on the icosahedra.[16]

C. Generation of liquid boron

Melting and equilibration were achieved by heating the solid configuration scaled at the liquid density using a 15 Ry electronic cutoff. The temperature was slowly increased to 2900 K and diffusive behavior was observed in the ionic trajectories. As the electronic system showed strong lack of adiabaticity, periodic electronic quenches were performed to force the electronic degrees of freedom onto the Born-Oppenheimer surface. Then, both electronic and ionic Nose's thermostats[17] were switched on and ionic temperature was stabilized at 2600 K. The fictitious mass associated with electronic degrees of freedom and thermostat were respectively 150 and 1440 a.u. to keep the fictitious kinetic energy around the value $E_{\rm kin}^{\rm target}=10^{-2}$ hartree. The mass of the ionic thermostat was set to 2×10^4 a.u., leading to the mean value $\langle T\rangle\sim2599$ K ($T^{\rm target}=2600$ K) when performing time averages as statistical averages in the canonical ensemble. The whole process took 1 ps. Finally, the plane wave cutoff was increased up to 35 Ry corresponding to approximately one hundred basis functions per atom.

After equilibrium, the system evolved for another picosecond with a time step $\Delta t\sim0.97\times10^{-16}$ s and statistics were performed (BHS results). The final atomic configuration was then used as a starting point to study liquid boron with the TM pseudopotential and a cutoff of 35 Ry. Before observing the system for another picosecond, we equilibrated the liquid by scaling ionic velocities and performing electronic quenches before switching the thermostats.

In both simulations, the atomic mean-square displacement was quasilinear. The self-diffusion coefficient was estimated either from the atomic mean-square displacement (D_1) or by means of the Green-Kubo formula (D_2). As a consequence of the less accurate electronic description, D_1 and D_2 differ by 10% in the BHS simulation and are highly consistent in the TM simulation (Table II).

TABLE II. Atomic self-diffusion coefficient in l-boron from atomic mean square displacement (D_1) or Green-Kubo formula (D_2). BHS (resp. TM) refers to the simulation using Bachelet-Hamann-Schlüter pseudopotential (resp. Trouiller-Martins pseudopotential).

Self-diffusion coeff.	$D_1\times10^4$(cm^{2}s^{-1})	$D_2\times10^4$(cm^{2}s^{-1})
BHS	1.68	1.85
TM	1.72	1.71

D. Pressure in the solid and in the liquid

In the simulation of the solid phase, the cell parameters are the experimental ones ($V_{\rm exp}=7.28$ Å^3/atom). As local-density approximation (LDA) underestimates the equilibrium volume by 3% [$V_{\rm eq}=7.05$ Å^3/atom (Ref. 8)], the system is slightly expanded in our simulation and the calculated[18] pressure at 0 K and $V_{\rm exp}$ is -7.3 GPa. As boron is a relatively hard material [experimental and theoretical bulk modulus are $B_{\rm exp}=224$ Gpa (Ref. 19) and $B_{\rm LDA}=249$ GPa (Ref. 8)], a small change in volume leads to an important value of the pressure in the solid.

In the liquid at the melting point, the isothermal bulk modulus is halved [estimation: 92 GPa (Ref. 2)]. During the simulation, the calculated mean electronic pressure at

the assumed density is −1 GPa at 2600 K after a correction of 14 GPa due to the Pulay stress.[20] Ionic thermal pressure is 4 Gpa, so that the total pressure is 3 GPa.

Nevertheless, no phase transition in crystalline boron is expected at this pressure.[21,6] As liquid-liquid phase transitions are usually related to phase transition in the solid, we therefore do not expect the calculated pressure in the melt to deeply modify the structural results.[21]

III. STRUCTURAL PROPERTIES AND BONDING PROPERTIES

A. Short-range order

It can be anticipated that covalency is affected by the disorder in liquid boron, and one may wonder which characteristic properties of the solid are still present in the liquid. The first such characteristic is the icosahedral unit. We checked, by just following labeled atoms, that there is no "molecular" liquid with an icosahedral unit and that any two atoms drift away in the course of the simulation.

Nevertheless, the icosahedral unit is also responsible for the low coordination number of solid boron, which can be computed by integrating the function $\rho 4\pi r^2 g(r)$ up to the position of the first minimum of the pair correlation function ($r_{max}=2.38$ Å).

The pair correlation function of the solid was generated by studying the phase at 700 K for 0.7 p [Fig. 3(a)]. In a unit cell, six atoms have an average coordination of 6 (five intraicosahedron neighbors and one intericosahedra two center bond) whereas the six remaining atoms have an average coordination of 7 because of the weak intericosahedra three-center bonds. This explains why the first shell is centered at 1.71 Å and leads to an average coordination of 6.5.

In the liquid [Fig. 3(a)], the first coordination shell is centered at the same distance 1.71 Å and the mean coordination number slightly decreases to 6 (TM: 5.9 atoms). The distribution of local coordination is broad. The liquid is composed of 35% sixfold, 25% fivefold, and 23% sevenfold coordinated atoms. In Table III, we have compared the positions of first and second neighbors shell and average coordination for the liquid, amorphous, α, and β rhombohedral phases. In the liquid, the first neighbor shell is slightly closer than in solid phases, whereas

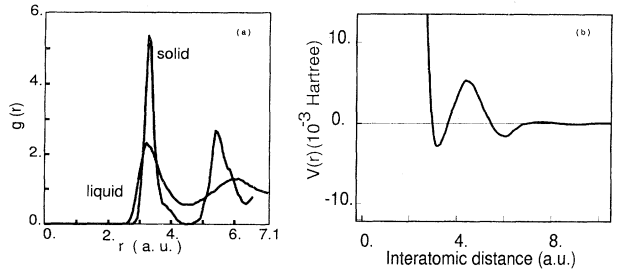

FIG. 3. (a) Pair correlation function of 1-boron and solid boron at 700 K (BHS results). (b) Effective pair potential in 1-boron computed as explained in the text. The small wiggles are due to the inherent noise in the method.[26]

TABLE III. Position of the maximum of the first neighbor shell (d_1) and second neighbor shell (d_2) in the pair distribution function of 1-boron, solid α-boron, and experimental β and amorphous phase. z is the first shell coordination number, and ρ the macroscopic density of the phase.[2] For the meaning of BHS and TM, see Table II.

Phase	d_1 (Å)	d_2 (Å)	z	T (K)	ρ(g cm^{-3})
Liquid (BHS)	1.71	3.18	6.0	2600	2.0
Liquid (TM)	1.69	3.12	5.9	2600	2.0
α rhomb.	1.71	2.86	6.5	700	2.46
β rhomb. (Ref. 36)	1.803	3.03	6.6	RT	2.35
Amorphous (Ref. 36)	1.833	3.05	6.4	RT	2.34

second neighbor shell is farther off. Average coordination is smaller in the liquid in comparison with all reported solid phases. Though metallic, the liquid has an open structure and the coordination is considerably lower than the minimal value $z \simeq 8$ that we would expect by analogy with metallic melt.[22]

The bond-angle distribution function $g(\theta, r_{max})$ represents the angle θ formed by nearest-neighbors bonds (i-j), (i-k) within a maximum length r_{max} around a central atom i.

First, r_{max} was chosen at the first minimum of $g(r)$ ($r_{max}=2.38$ Å), and results for the liquid and solid phases are superimposed on Fig. 4. In the solid phase, the main peaks around 60° and 108° originate from intraicosahedral bonds, i.e., when atoms j and k belong to the same icosahedron as atom i. The side peak at 126° occurs when i-k is a two center intericosahedral bond, and i-j an intraicosahedral bond. Finally, three-center intericosahedral bonds contribute to peaks at 60° and 108°, and give rise to peaks at 90° and 145°.

In the liquid, the bond-angle distribution still has two peaks, but as a consequence of disorder the bond angle distribution function is broadened and loses its structure. The angle at the first maximum is slightly shifted toward a lower value (56°).

We have then gradually reduced the maximum bond

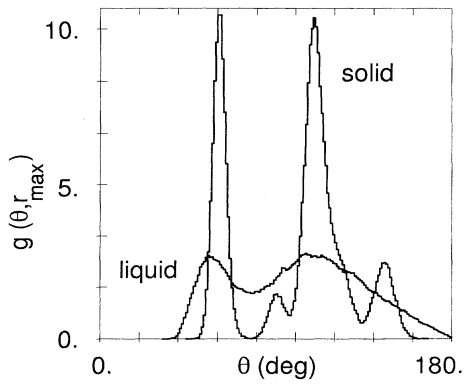

FIG. 4. Bond-angle distribution function $g(\theta, r_{max}=2.38$ Å) of 1-boron and solid boron at 700 K.

length r_{max} toward the first maximum of $g(r)$ (Fig. 5). At $r_{max}=1.98$ Å, the mean coordination number is 4 (5.5 in the solid). Shorter bonds (between 1.38 and 1.98 Å) have a small tendency to form larger angles (60°), but indeed, there are no qualitative changes in the shape of the distribution, in the sense that the ratio of the area of the two peaks is about the same. This seems to exclude the existence of a covalent radius, within which the local structure of the liquid would recall that of the solid, and favor the same coordination, as was found in liquid silicon by Stich, Car, and Parrinello.[23]

In order to shed some light on the nature of the low coordination in the liquid, we now turn to a more detailed study of the structural environment of sixfold coordinated atoms in solid and liquid phase (50% of the atoms, $r_{max}=2.38$ Å). The characteristic feature of the icosahedron in either solid phase is the pentagonal based pyramid.[24] More precisely, five neighbors $\{j_n,\ n=1,5\}$ of the sixfold coordinated atom i lie on a sphere and form a slightly distorted pentagon. The sixth-neighbor k belongs to another sphere in which it is at the top of another pentagonal-based pyramid. The two-center intericosahedral bond (i-k) then links two pentagonal-based pyramids.

We have searched for this type of structure in the liquid. We first isolated the neighbor (labeled k) which forms the largest angles with other first neighbors (labeled j_n). The bond angle distribution $j_n\hat{i}k$ is plotted on Fig. 6(a). This peaks at 120° in the solid and is shifted to the average value of 110° in the liquid. Then, in order to characterize the pentagonal-based pyramids, angles $(\sum_n \hat{j_n})ik$ were considered. $(\sum_n j_n)$ represents the vector $\sum_{n=1}^{5}(\mathbf{R}_{j_n}-\mathbf{R}_i)$ where $\mathbf{R}$ is the atomic position. Indeed, this distribution [Fig. 6(b)] peaks at 173° in the solid, but has a broad distribution round 152° in the liquid. The width at half-height is enlarged from 11° in the solid to 38° in the liquid. We conclude that there is no clear indication of the presence of pentagonal-based pyramids in the liquid.

Moreover, in our cell of 48 atoms, boron solid is

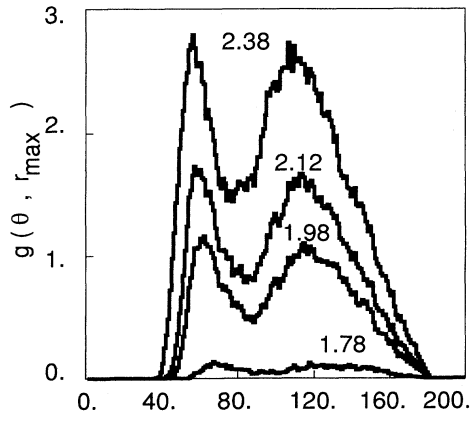

FIG. 5. Bond-angle distribution function $g(\theta, r_{max})$ at various cutoff distances r_{max} in 1-boron.

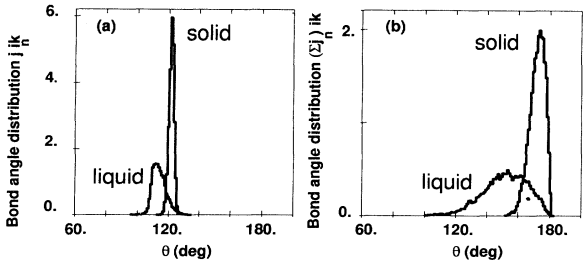

FIG. 6. Characterization of the first neighbor shell of the sixfold coordinated atoms i in solid and liquid phase. In the solid, j_n and i belongs to the same sphere, and k to another icosahedron. (a) Distribution of the maximum bond angles $j_n\hat{i}k$ between first neighbors of atom i, i.e., between external bond j-k and internal bond i-j_n. (b) Distribution of bond angles between external bond i-k and the sum of the vectors along pyramid edges $\sum_{n=1}^{5}(\mathbf{R}_{j_n}-\mathbf{R}_i)$.

formed by 80 intraicosahedral bonds. As two-center intericosahedral bonds are stronger than intraicosahedral ones, we have investigated the liquid to know in what proportion the later type of bond still exists. We therefore investigated the underlying electronic density. It is strongly nonuniform with an accumulation between pairs of atoms. We selected triangular atomic arrangements in the liquid by means of reduced coordinates constructed in the three-body configuration space[25] and studied the electronic density in the plane of these arrangements. Compared to the solid, the liquid only contains between 5 and 15% of three-center bonds. Although atomic volume increases from 7.28 to 7.55 Å^3/atom, they involve maxima of density (140–170 me/a_0^3) stronger than that of the intraicosahedral bonds of the solid (128 me/a_0^3) by at least 10%. Figure 7 shows patterns of electronic pseudodensity found in the final liquid. Atomic cores appear as spherical density holes within clusters, as pseudopotential formalism only describes valence orbitals.

Thus, although mean coordination is about the same in the liquid and solid phases, the electronic bonding and then the atomic structure are substantially changed on melting, and that explains the pronounced semiconductor to metal transition in boron.

B. Corresponding effective pair potential

There has been a lot of speculation about the shape of an effective pair potential for boron, as it is well known that second order perturbation theory is inadequate. To get an idea of the effective interaction between boron atoms, we inverted the simulated pair correlation function using the predictor-corrector method described by Reatto, Levesque, and Weis.[26] The pair correlation function was extended using the Orstein-Zernike relation, assuming that for r larger than half the simulation box length, the direct correlation function was zero.

The resulting potential [Fig. 3(b)] displays a strong oscillation of wavelength $\lambda_F=\pi/k_F=2.76$ a.u., the Friedel

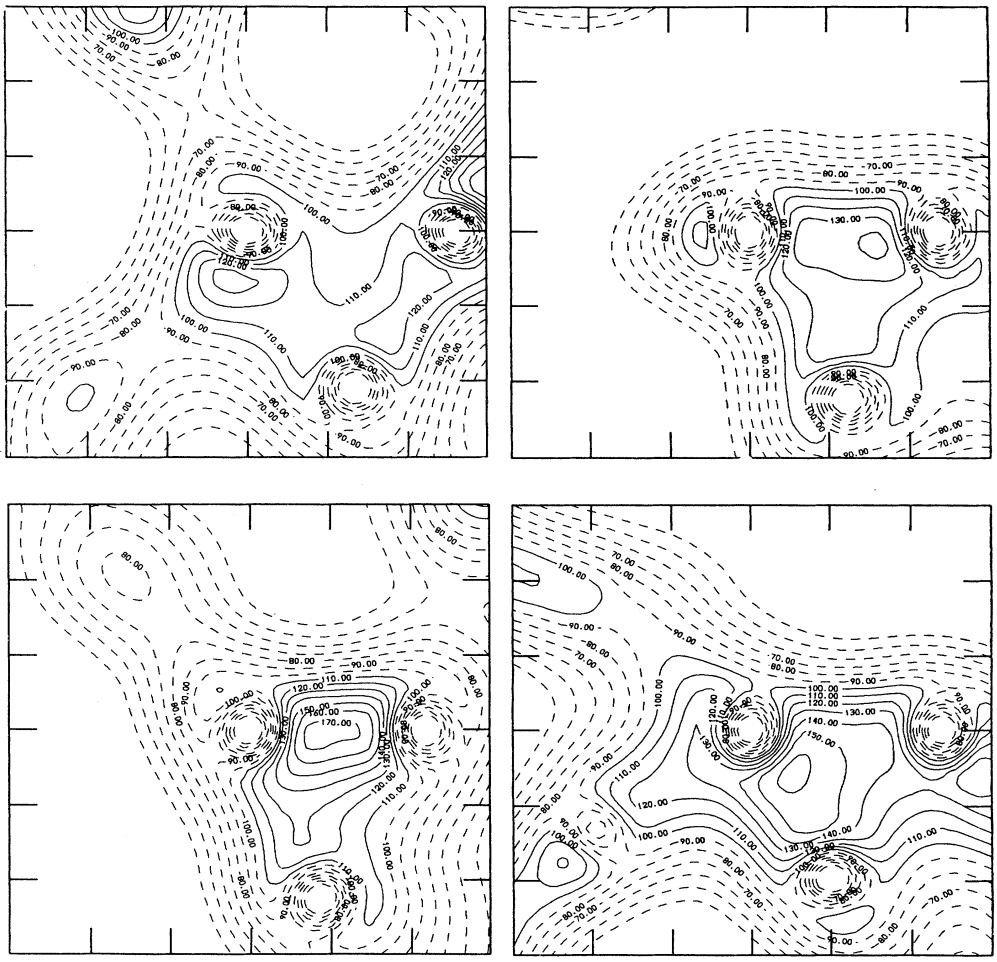

FIG. 7. Isovalues of the electronic charge density in steps of 10 me/a_0^3 for various three-body atomic configurations at the end of the simulation. Density is expressed in me/a_0^3.

wavelength, which tends to split the compact nearest neighbors shell and form an open structure. While the strong minimum at about λ_F was accurately predicted by Ref. 27, the amplitude of the oscillation appears underestimated. This effective potential reproduces qualitatively the bond-angle distribution function (Fig. 8) and, therefore, the main characteristics of the liquid structure come from the nearest-neighbor shell splitting, which is accounted for in our effective potential.

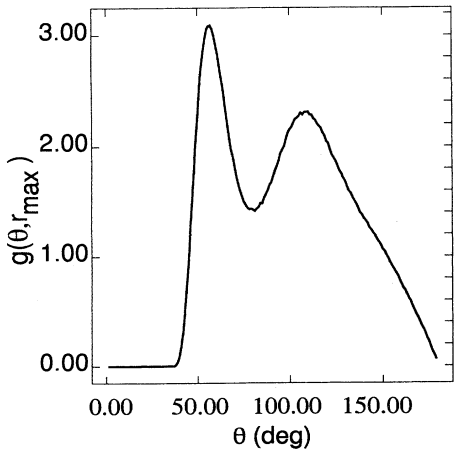

FIG. 8. Bond-angle distribution function calculated with the effective pair potential of Fig. 3(b) by a 68-particles Monte-Carlo simulation.

IV. DYNAMICAL PROPERTIES

We now turn to atomic dynamical properties. The values of the self-diffusion coefficient have been given in Sec. II C, and we now consider the velocity autocorrelation function $\tilde{Z}(t)$ [Fig. 9(a), TM pseudopotential]. Its fast decay is related to the low compressibility of boron in the liquid phase. Indeed, the short-time expansion of $\tilde{Z}(t)$:

$$\tilde{Z}(t)=\frac{k_B T^{\text{target}}}{M_I}\left[1-\Omega_0^2\frac{t^2}{2}+\cdots\right] \tag{1}$$

leads to an estimated value for Ω_0 of 11.10^{13} s^{-1}, which is large compared to the value obtained for other liquid [for instance, in argon, $\Omega_0^{\text{Ar}}\sim 10^{13}$ s^{-1} (Ref. 28)]. The mean squared force exerted on a diffusing particle by its neighbors in liquid boron is therefore much larger than in other liquids.

Moreover, for times greater than 1.8×10^{-2} ps, $\tilde{Z}(t)$ presents an extended negative region. This is caused by the caging effect of the neighboring particles over a

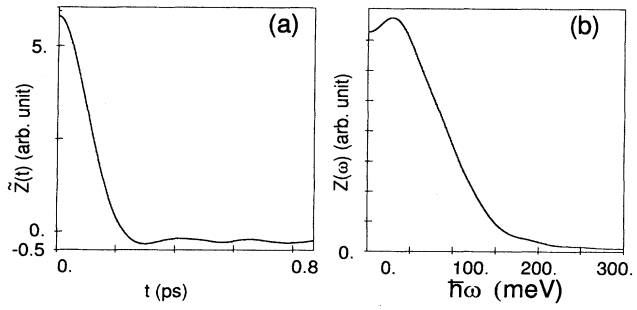

FIG. 9. (a) Velocity autocorrelation function for plane-wave cutoff of 35 Ry (TM). (b) The power spectrum convoluted with a triangular window.

diffusing atom in the rather open but less compressible liquid boron. The negative region in the velocity autocorrelation function explains the behavior of the power spectrum $Z(\omega)$, whose convolution with a triangular window is shown on Fig. 9(b) (TM pseudopotential). A maximum appears at a frequency around 30 meV. This is not related to a collective vibratory motion, as we found no indication of a side peak in the dynamical structure factor within the range of wave vectors accessible in our simulation ($k > 0.88$ Å^{-1}).[29]

The velocity autocorrelation function is quite sensitive to plane wave basis incompleteness. We have observed the boron system for another 0.8 ps with an energy cutoff of 15 Ry and the BHS pseudopotential. We found slight differences on the pair correlation function, but, for instance, the coordination numbers were the same. Whereas no difference was observed in the short time correlations of $Z(t)$ (same mean squared force in both cases), no anticorrelation region was observed at 15 Ry (Fig. 10; BHS results).

V. ELECTRONIC PROPERTIES

A. Electronic density of states

A comparison of the liquid and solid density of states (DOS) is somewhat problematic since the liquid DOS is

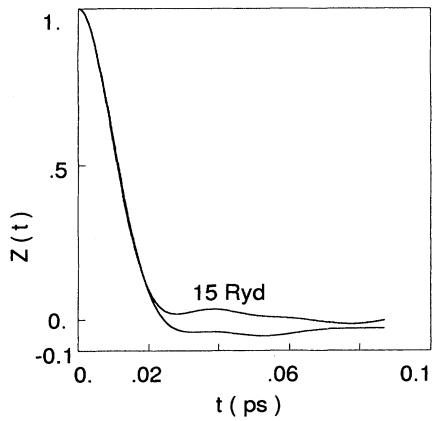

FIG. 10. Normalized velocity autocorrelation function for 15 and 35 Ry with BHS pseudopotential (see text).

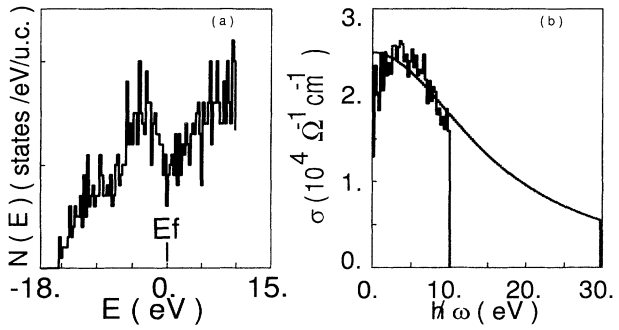

FIG. 11. (a) Single particle electronic density of states and (b) corresponding electronic conductivity $\sigma(\omega)$. The dotted line is the Drude fit. Electronic data were averaged over eight ionic configurations (BHS results).

computed with the Γ point only. This leads to artifacts such as bumps in the DOS,[30] and the appearance of a peudogap at the Fermi level. Presumably, as for other elemental liquids of column IV in the Periodic Table, this will be smoothed by the inclusion of more **k** points in the Brillouin zone or by the use of the larger simulation cell.

The computed density of states [Fig. 11(a)] shows nearly-free-electron–like behavior which explains our observation of a Friedel wavelength modulation in the effective potential. Liquid boron is metallic whereas amorphous or rhombohedral phases are semiconducting with a gap of the order of 2 eV. The semiconducting properties come from the peculiar icosahedral arrangement. Indeed, all hypothetical phases studied by Mailhot *et al.*, and based on different atomic arrangement, are metallic. On melting, atomic structure is profoundly modified and the liquid has a high conductivity.

The details of the solid DOS, such as the cluster level at about -15 eV, which is very distinct from the rest of the band in the solid,[16] vanishes in liquid state, but the bandwidth (15 eV) compares with solid state values. Indeed, according to x-ray emission experiments, valence band in amorphous, α, and β rhombohedral boron are respectively 16, 15.5, and 15.8 eV wide.[15]

B. Electrical conductivity

A rough estimate of the ionic conductivity by means of Einstein formula yields $\sigma_I = 76\Omega^{-1}\,\mathrm{cm}^{-1}$. We then used Kubo-Greenwood formula to estimate electronic conductivity [Fig. 11(b)] arising from transitions between occupied and empty states:

$$\sigma(\omega)=\frac{\pi c^2}{3\ \Omega\ \mathrm{m}^2}\sum_{i=x,y,z}\sum_{\alpha,\beta}|\langle\alpha|p_i|\beta\rangle|^2 \times\frac{(f_\alpha-f_\beta)}{\omega_{\alpha,\beta}}\delta(\hbar\omega-\varepsilon_{\alpha,\beta})\ . \quad (2)$$

We have assumed the occupation numbers f_α to be given by 0 K Fermi distribution and neglected corrections to momentum matrix elements arising from noncommutation of the position operator and the nonlocal part of pseudopotential. Restricted number of excited eigen-

states does not allow to determine the conductivity above 10 eV.

A Drude's law fits the theoretical result within the frequency range and yields the static conductivity $\sigma_{dc} \sim 2.5 \times 10^4\ \Omega^{-1}\,cm^{-1}$ and an inverse relaxation time $\hbar\tau_D^{-1} = 16$ eV. A careful analysis of the pseudo wave functions around the Fermi level shows that they are spatially very extended and this gives rise to the high value of σ_{dc}.

In the absence of experimental data, a lower bound for dc conductivity may be deduced from the experimental fact that liquid boron can be heated by electromagnetic induction at 450 kHz: $0.5 \times 10^4\ \Omega^{-1}\,cm^{-1}$.[31] We may also estimate an upper bound from Allgaier's work on electronically conducting liquid as being $10^5\ \Omega^{-1}\,cm^{-1}$.[32]

On the other hand, Rinker[33] used an extension of Ziman formula to compute transport coefficients in plasmas. Although the model cannot give a reliable quantitative result for a liquid near melting, the approximation can give a lower bound for the static conductivity, depending on the estimated ionization. At the density $\rho \simeq 2.08\ g\,cm^{-3}$ and the temperature $T \simeq 2900$ K, a lower bound for the conductivity of liquid boron in this simple model is $\sigma \simeq 2.4 \times 10^4\ \Omega^{-1}\,cm^{-1}$,[34] in accordance with our *ab initio* values.

VI. CONCLUSION

In summary, we have presented a careful *ab initio* molecular-dynamics study of liquid boron, which settles some conjectures despite the small number of particles. When solid boron melts, average atomic structural properties tend to an open packing with sixfold coordination but the atomic structure is profoundly modified. Indeed, pentagonal-based pyramids characteristic of the icosahedron are destroyed. The subtle covalent bonds which make solid phases semiconducting therefore disappear, and we found a free electron like density of states which leads to a high electrical conductivity in the melt.

ACKNOWLEDGMENTS

We would like to thank R. Car who gave us the computer program, P. Dallot, G. Galli, K. Laasonnen, G. Pastore, J. Penman, and S. Rabii for fruitful discussions from which this work has benefited. We thank R. Pollack for the critical reading of the manuscript.

*Electronic address: vast@limeil.cea.fr

[1]F. A. Cotton and G. Wilkinson, *Advanced Inorganic Chemistry* (Wiley, New York, 1988).
[2]K. C. Buschbeck, *Boron Compounds, Elemental Boron and Boron Carbides,* Gmelin Handbook of Inorganic Chemistry Vol. 13 (Springer, Berlin, 1981), Suppl. 2.
[3]S. Krishnan, P. C. Nordine, J. K. R. Weber, and R. A. Schiffman, High Temp. Sci. **31**, 45 (1991).
[4]E. Amberger and K. Ploog, J. Less Common Met. **23**, 21 (1971).
[5]S. Lee, D. M. Bylander, S. W. Kin, and L. Kleinman, Phys. Rev. B **45**, 3248 (1992).
[6]D. A. Young, *Phase Diagrams of the Elements* (University of California, Berkeley, 1991).
[7]D. Emin, Phys. Today **40**, 55 (1987).
[8]C. Mailhiot, J. B. Grant, and A. K. McMahan, Phys. Rev. B **42**, 9033 (1990).
[9]J. Hafner and V. Heine, J. Non-Cryst. Solids **117/118**, 308 (1990).
[10]D. V. Khantadze and N. J. Topuridze, J. Less Common Met. **117**, 105 (1986).
[11]S. H. Tsagareishvili and G. V. Tsagareishvili, J. Less Common Met. **67**, 541 (1979).
[12]R. Stumpf, X. Gonze, and M. Scheffler (unpublished).
[13]N. Trouiller and J. L. Martins, Phys. Rev. B **43**, 1993 (1991).
[14]G. Loupias, R. Wentzcovitch, L. Bellaiche, J. Moscovici, and S. Rabii, Phys. Rev. B **49**, 13 342 (1994).
[15]E. P. Domashevskaya, N. E. Solovjev, V. A. Terekhov, and Y. A. Ugai, J. Less Common Met. **47**, 189 (1974).
[16]S. Lee, D. M. Bylander, and L. Kleinman, Phys. Rev. B **42**, 1316 (1990).
[17]P. E. Blöchl and M. Parrinello, Phys. Rev. B **45**, 9413 (1992).
[18]O. H. Nielsen and R. M. Martins, Phys. Rev. B **32**, 3780 (1985).
[19]R. J. Nelmes, J. S. Loveday, D. R. Allan, J. M. Besson, G. Hamel, P. Grima, and S. Hull, Phys. Rev. B **47**, 13 (1993).
[20]D. Vanderbilt, Phys. Rev. Lett. **59**, 1456 (1987).
[21]A. C. Mitus and A. Z. Patashinskii, Acta Phys. Pol. A **74**, 779 (1988).
[22]Y. Wasdea, *The Structure of Non-Crystalline Materials* (McGraw-Hill, New York, 1980).
[23]I. Stich, R. Car, and M. Parrinello, Phys. Rev. B **44**, 4262 (1991).
[24]D. W. Bullett, in *Boron-Rich Solids,* edited by D. Emin, T. Aselage, C. L. Beckel, I. A. Howard, and C. Wood, AIP Conf. Proc. No. 140 (AIP, New York, 1986), p. 249.
[25]P. Dallot, P. D. Bristowe, and M. Demazure, Phys. Rev. B **46**, 2133 (1992).
[26]L. Reatto, D. Levesque, and J. J. Weis, Phys. Rev. A **33**, 3451 (1986).
[27]J. Hafner and V. Heine, J. Phys. F **13**, 2479 (1983).
[28]J. P. Hansen and I. R. McDonald, *Theory of Simple Liquids* (Academic, New York, 1986).
[29]J. R. D. Copley and S. W. Lovesey, Rep. Prog. Phys. **38**, 461 (1975).
[30]W. Jank and J. Hafner, Phys. Rev. B **41**, 1497 (1990).
[31]J. K. R. Weber (private communication).
[32]R. S. Allgaier, Phys. Rev. **185**, 227 (1969).
[33]G. A. Rinker, Phys. Rev. B **31**, 4207 (1985).
[34]G. A. Rinker (unpublished).
[35]B. F. Decker and J. S. Kasper, Acta Cryst. **12**, 503 (1959).
[36]R. G. Delaplane, T. Lundstrom, U. Dahlborg, and W. S. Howells, in *Boron-Rich Solids,* edited by D. Emin, T. L. Aselage, A. C. Switendick, and C. L. Beckel, AIP Conf. Proc. No. 231 (AIP, New York, 1991), p. 241.